DNA Abasic Lesions in a Different Light: Solution Structure of an Endogenous Topoisomerase II Poison†

Susan D. Cline,‡ Wendelyn R. Jones,§,|| Michael P. Stone,§ and Neil Osheroff*,‡,⊥

From the Departments of Biochemistry and Medicine (Hematology), Vanderbilt University School of Medicine, Nashville Tennessee 37232-0146, and the Department of Chemistry and Center in Molecular Toxicology, Vanderbilt University, Nashville Tennessee 37235

Received July 28, 1999; Revised Manuscript Received September 23, 1999

ABSTRACT: Topoisomerase II is the target for several anticancer drugs that "poison" the enzyme and convert it to a cellular toxin by increasing topoisomerase II-mediated DNA cleavage. In addition to these "exogenous topoisomerase II poisons," DNA lesions such as abasic sites act as "endogenous poisons" of the enzyme. Drugs and lesions are believed to stimulate DNA scission by altering the structure of the double helix within the cleavage site of the enzyme. However, the structural alterations that enhance cleavage are unknown. Since abasic sites are an intrinsic part of the genetic material, they represent an attractive model to assess DNA distortions that lead to altered topoisomerase II function. Therefore, the structure of a double-stranded dodecamer containing a tetrahydrofuran apurinic lesion at the +2 position of a topoisomerase II DNA cleavage site was determined by NMR spectroscopy. Three major features distinguished the apurinic structure ($R_1^x = 0.095$) from that of wild-type ($R_1^x = 0.077$). First, loss of base stacking at the lesion collapsed the major groove and reduced the distance between the two scissile phosphodiester bonds. Second, the apurinic lesion induced a bend that was centered about the topoisomerase II cleavage site. Third, the base immediately opposite the lesion was extrahelical and relocated to the minor groove. All of these structural alterations have the potential to influence interactions between topoisomerase II and its DNA substrate.

Topoisomerase II is an essential enzyme that participates in virtually every aspect of DNA metabolism. It plays fundamental roles in DNA replication, transcription, and recombination and is required for chromosome segregation and the maintenance of proper chromosome structure (*1*−*4*).

As a requirement for its critical catalytic functions, topoisomerase II creates transient double-stranded breaks in the backbone of DNA (*1, 2, 4, 5*). During this cleavage event, topoisomerase II maintains the continuity of the genetic material by forming covalent bonds between its two active site tyrosyl residues (one per subunit of the homodimeric enzyme) and the 5′-termini of the cleaved DNA (*6*−*9*). Normally, this covalent enzyme-DNA "cleavage complex" is a fleeting intermediate in the catalytic cycle of topoisomerase II and is tolerated by the cell (*1, 2, 4, 10*). However, conditions that significantly increase physiological levels of topoisomerase II-associated DNA breaks lead to the formation of mutations and chromosomal aberrations, and in some cases, initiate pathways that culminate in cell death (*11*−*15*). Therefore, because of its DNA cleavage activity, topoisomerase II assumes a dual persona: while essential to cell viability, the enzyme poses an intrinsic threat to genomic integrity.

Agents that stimulate topoisomerase II-mediated DNA cleavage are referred to collectively as "topoisomerase II poisons" because they convert this required enzyme into a potential cellular toxin (*16, 17*). Exogenous topoisomerase II poisons have important clinical applications. Drugs such as etoposide, doxorubicin, and mitoxantrone represent some of the most successful agents used to treat human cancers (*4, 10, 13, 17*−*21*). Furthermore, quinolones (which target prokaryotic type II topoisomerases) are the most active and broad spectrum class of antibacterials currently available (*22*−*24*). Although topoisomerase II-targeted drugs differ in structure, they all are believed to act at the enzyme−DNA interface and stimulate cleavage by altering the structure of the DNA within the active site of the enzyme (*4, 13, 25*−*28*).

In addition to these exogenous poisons, recent evidence indicates that several forms of DNA damage act as endogenous topoisomerase II poisons (*28*). Of these, apurinic lesions are the most efficacious (*28*−*32*). When located within the 4-base overhang generated by topoisomerase II-mediated scission, apurinic sites stimulate DNA cleavage as much as 20-fold and are ∼1000 times more potent than drugs such as etoposide (*28*−*30, 33*).

† This work was supported by NIH Grants GM53960 (N. O.), CA55678 (M. P. S.), and RR05805 and ES00267 (NMR Facility). S. D. C. was a trainee under NIH Grant GM08320.

‡ Department of Biochemistry, Vanderbilt University School of Medicine.

§ Department of Chemistry and Center in Molecular Toxicology, Vanderbilt University.

|| Present address: Department of Bioengineering and Environmental Health, Massachusetts Institute of Technology, Cambridge, Massachusetts 02139.

⊥ Department of Medicine, Vanderbilt University School of Medicine.

* To whom reprint requests should be addressed. Telephone: 615-322-4338. Fax: (615) 343-1166. E-mail: osheron@ctrvax.vanderbilt.edu.

10.1021/bi991750s CCC: $18.00
Published on Web 11/02/1999

Despite the importance of topoisomerase II poisons to the treatment of human malignancies and their potential threat to genomic stability, the mechanism by which they stimulate enzyme-mediated DNA scission is not well understood. Two of the most important issues yet to be resolved are: (1) what alterations in nucleic acid structure are induced by poisons and (2) how do these structural perturbations enhance the cleavage activity of topoisomerase II? Unfortunately, the necessary studies with exogenous poisons present a formidable challenge, since they require crystallography of a ternary topoisomerase II−DNA−drug complex. In contrast, because lesions are an intrinsic part of the DNA helix, they represent an attractive and tractable model to assess distortions in the genetic material that may lead to altered topoisomerase II function.

Therefore, in the present study, we characterized the features of apurinic sites that contribute to their actions as topoisomerase II poisons and utilized NMR spectroscopy to determine the solution structure of a topoisomerase II DNA cleavage sequence that contained an apurinic lesion. Results indicate that the endogenous poison collapsed the major groove in the cleavage site, which in turn reduced the distance between the scissile bonds and induced a bend in the DNA backbone. These data provide our first look at the structural distortions in DNA that may lead to enhanced cleavage by topoisomerase II.

EXPERIMENTAL PROCEDURES

Preparation of Oligonucleotides. A 42-base single-stranded oligonucleotide that corresponds to residues 1050−1091 of the *MLL* oncogene (*34*), and its complementary oligonucleotide were synthesized. The sequences of the top and bottom oligonucleotides were 5′-ATGATTGTACCA-CTGCAG↓TCCAGCCTGGGTG ACAAAGCAAAA-3′ and 5′-TTTTGCTTTGTCACCCAGGC↓TGGACTGCAGTGG-TA CAATCAT- 3′, respectively. Points of topoisomerase II-mediated DNA cleavage are denoted by arrows (*34*, *35*). Modified bottom oligonucleotides containing a deoxyuridine, a tetrahydrofuran abasic site analogue (Cruachem, Aston, PA), or a three carbon spacer (Glen Research, Sterling, VA) were synthesized using the corresponding phosphoramidite. For DNA cleavage assays, single-stranded oligonucleotides were [^{32}P]-labeled on their 5′-termini with T4 polynucleotide kinase, purified by electrophoresis on a 7 M urea/14% polyacrylamide gel, visualized by UV shadowing, excised, and eluted using the QIAGEN gel extraction protocol. Complementary oligonucleotides were annealed by incubating equimolar amounts at 70 °C for 10 min and cooling to 25 °C (*35*). To generate a natural abasic site, the annealed oligonucleotide containing a uracil was treated with *Escherichia coli* uracil DNA glycosylase (0.5 U/2 pmol oligonucleotide) in 70 mM Hepes-HCl (pH 7.9), 0.35 mM EDTA, and 8.75% glycerol at 37 °C for 30 min. The reaction was desalted using a Bio-Spin 6 column. To generate the reduced deoxyribitol analogue, the abasic oligonucleotide was treated with 100 mM $NaBH_4$ in 40 mM KP (pH 6.5) at 25 °C for 1 h.

Topoisomerase II-mediated DNA Cleavage. Human topoisomerase IIα was purified from *Saccharomyces cerevisiae* as described (*35*). DNA cleavage reactions contained 100 nM oligonucleotide in 10 mM Hepes-HCl (pH 7.9), 0.1 mM EDTA, 100 mM KCl, 5 mM $MgCl_2$, and 2.5% glycerol and were initiated by the addition of human topoisomerase IIα (150 nM final concentration). Reactions were incubated at 37 °C for 10 min and stopped by the addition of SDS (1% final concentration) and EDTA (16 mM final concentration). When appropriate, cleavage reactions were reversed by the addition of NaCl (500 mM final concentration) at 37 °C for 5 min prior to the addition of detergent and EDTA. Cleavage products were digested with proteinase K, precipitated with ethanol, and resolved by electrophoresis in denaturing 7 M urea/14% polyacrylamide gels. Reaction products were visualized and quantified using a Molecular Dynamics PhosphorImager system. Cleavage was monitored on the complementary wild-type strand. Levels of DNA scission were calculated relative to that obtained with the wild-type substrate.

NMR Spectroscopy. Single-stranded oligonucleotides purified by anion exchange chromatography were obtained from Midland Certified Reagent Co. (Midland, TX). Sequences of the complementary strands were 5′-GCAG↓TC CAGCCT-3′ and 5′-AGGC↓TXGACTGC-3′, where X is G or the tetrahydrofuran analogue and arrows denote the points of topoisomerase II-mediated cleavage. Dodecamers were annealed as described above, purified by hydroxylapatite chromatography, and desalted on G-25 resin. All NMR data were collected at 20 ± 0.5 °C on Bruker instruments. One-dimensional ^{1}H NMR data for both duplexes and T1 data for the abasic duplex were collected at 400 MHz. Two-dimensional ^{1}H NMR spectral data were collected for both oligodeoxynucleotides at 500 MHz (*36*, *37*). Each duplex was dissolved in 0.5 mL of 10 mM sodium phosphate (pH 7.0), 100 mM NaCl, 50 μM Na_2EDTA, exchanged 3 times with 99.9% D_2O, and resuspended in 99.96% D_2O (∼150 A_{260} units/0.5 mL). Phase-sensitive NOESY data, used for assignment of nonexchangeable protons, were collected at experimental mixing times of 150, 250, and 350 ms for the wild-type duplex and 80, 150, 250, and 350 ms for the abasic duplex (*36*, *37*). A DQF−COSY[1] spectrum was run for the abasic DNA sample to confirm sugar proton cross-peak assignments. To observe exchangeable protons (τ_m = 250 ms), the abasic dodecamer was lyophilized and resuspended in 9:1 H_2O/D_2O (*36*, *37*). Spectral data from the NOESY and DQF−COSY experiments were processed and peak volumes for calculating NOE intensities were measured using FELIX 3.1 and FELIX 97 (Molecular Simulations, San Diego, CA) running on Indigo2 and Octane workstations (Silicon Graphics, Mountain View, CA).

Distance Measurements and Molecular Dynamics. A-DNA (*38*) and B-DNA (*38*, *39*) starting structures for each duplex were built with INSIGHTII (Molecular Simulations) and potential energy minimized to obtain IniA and IniB. For each of the three longer mixing times, a hybrid intensity matrix of experimental intensities supplemented with calculated intensities from IniB was constructed using MARDIGRAS (*40*). RMA using CORMA yielded internuclear distances (*41*). A total of 345 wild-type and 365 abasic dodecamer

[1] Abbreviations: NMR, nuclear magnetic resonance; NOE, nuclear Overhauser enhancement; NOESY, two-dimensional nuclear Overhauser enhancement spectroscopy; DQF−COSY, double quantum filtered-homonuclear 2D correlated spectroscopy; RMA, relaxation matrix analysis; rmsd, root-mean-square deviation; T1, longitudinal relaxation time.

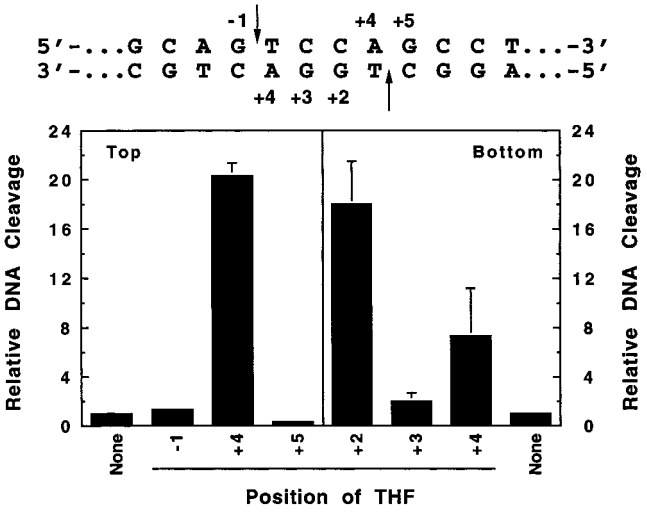

FIGURE 1: Effects of position-specific apurinic lesions on DNA cleavage mediated by human topoisomerase IIα. A tetrahydrofuran abasic site analogue was incorporated at the specified positions on the top and bottom strands. Data represent the average of three independent experiments. Standard deviations are indicated by error bars.

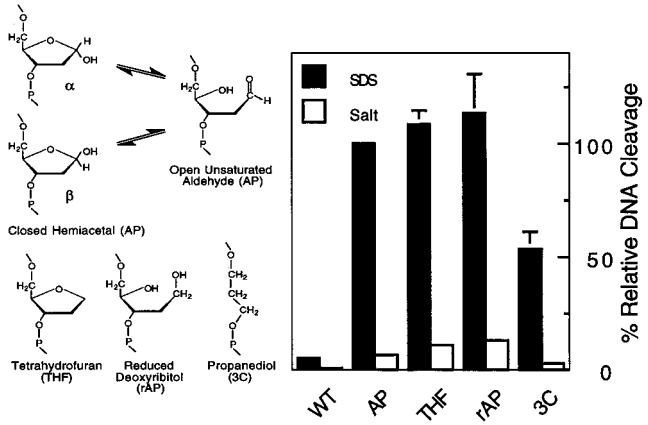

FIGURE 2: Effects of the apurinic sugar structure on DNA cleavage mediated by human topoisomerase IIα. A natural apurinic lesion (*AP*), tetrahydofuran (*THF*), and reduced deoxyribitol (*rAP*) analogues, and a three carbon linker (*3C*) are depicted at *left*. Each was incorporated at the +2 bottom strand position of the topoisomerase II DNA cleavage site shown in Figure 1. Levels of DNA cleavage obtained with each structural analogue are reported relative to that obtained with the natural lesion (set to 100%). Data represent the average of three independent experiments. Standard deviations are indicated by error bars.

NOE distance constraints were determined. Restrained molecular dynamics calculations using XPLOR yielded emergent structures for which convergence was monitored by calculating pairwise root-mean-square deviation (*37, 42, 43*). Accuracy was assessed by RMA using CORMA (*37, 43*). The refined structures were analyzed using DIALS AND WINDOWS 1.0 (*44*).

RESULTS AND DISCUSSION

Drugs that increase levels of topoisomerase II-mediated DNA cleavage have been used for the treatment of human cancers and infections for over two decades (*4, 10, 13, 17*−*21*). Despite their clinical importance, the mechanistic basis for their actions against the enzyme has not been fully described. Recent evidence indicates that topoisomerase II poisons stimulate DNA cleavage by altering the structure of the double helix proximal to the points of scission (*4, 13, 25*−*28*). However, the nature of this distortion is unknown.

Abasic lesions in DNA are position-specific topoisomerase II poisons and stimulate DNA scission when they are located within the 4-base cleavage overhang created by the enzyme (*28*−*30, 35*). Since these lesions are a component of the double helix, they represent a compelling system in which to characterize the alterations in DNA structure induced by topoisomerase II poisons.

Positional Preference of Human Topoisomerase IIα for Apurinic Lesions Within a DNA Cleavage Sequence. Of the DNA lesions examined, apurinic sites display the greatest ability to stimulate topoisomerase II-mediated DNA scission (*28*−*30*). Therefore, as a first step toward assessing the structural distortions in DNA that lead to altered topoisomerase II function, we determined the positional preference of human topoisomerase IIα for apurinic lesions located within a drug-inducible DNA cleavage site. The substrate utilized for this study was a 42 bp oligonucleotide that contained a centrally located cleavage site for human topoisomerase IIα (Figure 1). The sequence was derived from a region of the *MLL* oncogene proximal to a leukemic breakpoint at chromosomal band 11q23 (*34*). Individual substrates contained single tetrahydrofuran apurinic site analogues incorporated at the indicated positions.

Apurinic lesions located between the points of scission (+2, +3, and +4 positions) stimulated topoisomerase II-mediated DNA scission up to 20-fold (Figure 1). In contrast, those located immediately outside the cleavage site showed little or no enhancement. These results are consistent with previous findings on the positional specificity of type II topoisomerases for DNA lesions (*28*−*30, 35*). The greatest increase in DNA cleavage was observed when an apurinic site was incorporated at the +4 position on the top strand or the +2 position on the bottom. Since +2 lesions consistently induce high levels of DNA cleavage in other sequences examined (*28*−*30, 35*), oligonucleotides containing an apurinic site at the +2 position of the bottom strand were used for all subsequent experiments.

Effects of the Apurinic Sugar on Topoisomerase II-mediated DNA Cleavage. In natural apurinic lesions, the remaining deoxyribose sugar exists in equilibrium between a closed (hemiacetal) and open (unsaturated aldehyde) form (Figure 2). Normally, this equilibrium lies heavily (∼99%) toward the hemiacetal (*45*).

To characterize potential requirements for the apurinic sugar, we assessed the ability of human topoisomerase IIα to cleave substrates that contained a natural apurinic site or three apurinic analogues at the +2 position: a tetrahydrofuran (which models the hemiacetal), a reduced deoxyribitol (which models the unsaturated aldehyde), or a propanediol spacer (which models the loss of the sugar). Results are shown in Figure 2. In all cases, cleavage was reversed by the addition of salt, indicating that DNA scission of these apurinic substrates was mediated by topoisomerase II (*29, 30, 35*).

Human topoisomerase IIα appears to be relatively insensitive to the structure of the apurinic sugar. Indeed, the tetrahydrofuran and reduced deoxyribitol analogues both displayed high levels of DNA cleavage enhancement that were comparable to those of the natural apurinic site. However, less DNA cleavage enhancement was observed

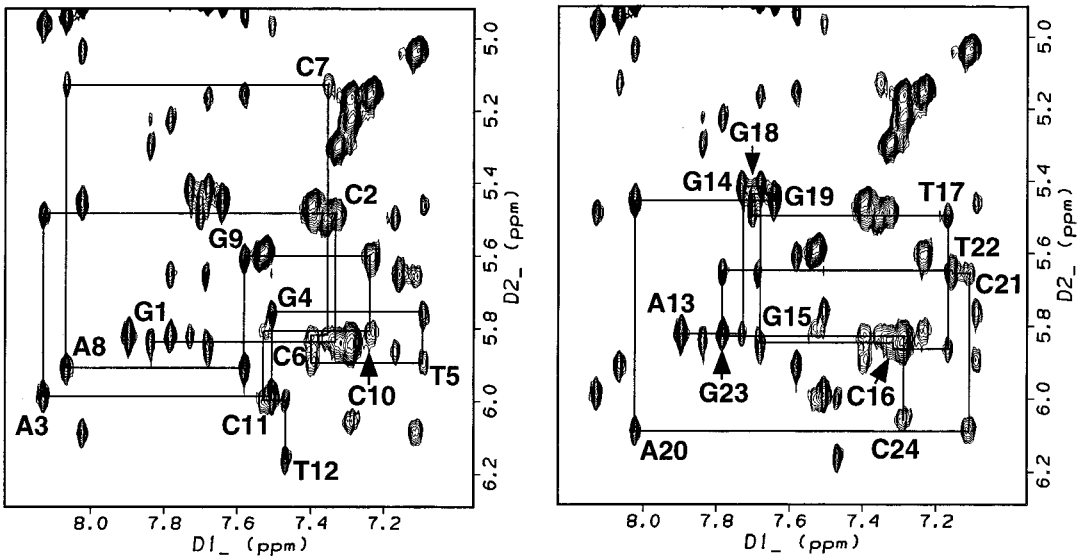

FIGURE 3: Expanded plot of a phase-sensitive NOESY spectrum of the wild-type dodecamer in D_2O buffer collected with a mixing time of 250 ms. The traces represent sequential NOE connectivities from the aromatic to H1′ protons for the top strand (*left panel*) and the bottom strand (*right panel*) residues of the oligodeoxynucleotide.

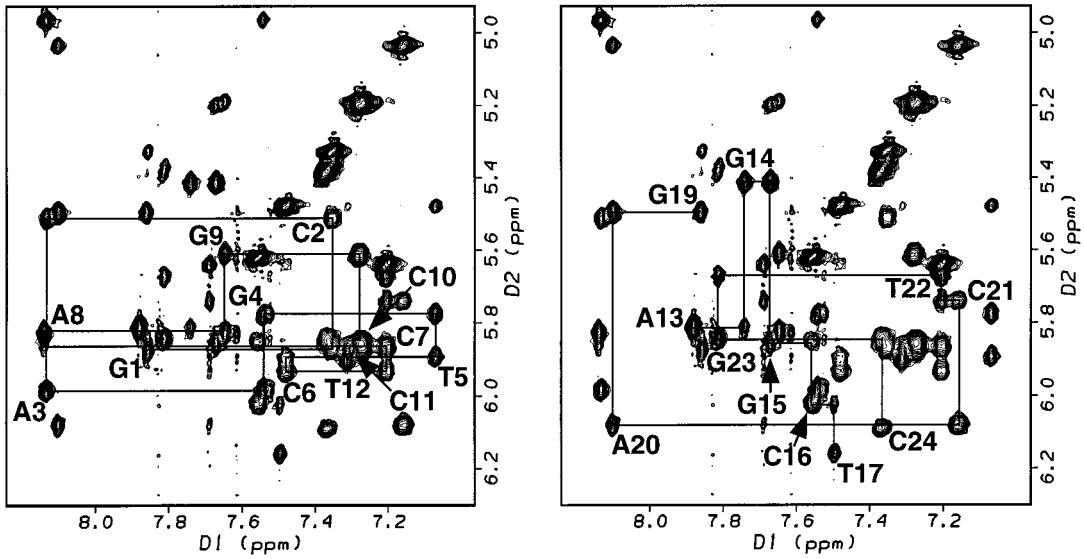

FIGURE 4: Expanded plot of a phase-sensitive NOESY spectrum of the apurinic dodecamer in D_2O buffer collected with a mixing time of 250 ms. The traces represent sequential NOE connectivities from the aromatic to H1′ protons for the top strand (*left panel*) and the bottom strand (*right panel*) residues of the oligodeoxynucleotide. A break in NOE connectivity between residues T17 and G19 confirms the loss of the +2 guanine at postition 18 on the bottom strand.

when the deoxyribose moiety was replaced by a propanediol spacer. Thus, it seems that the presence of the sugar heightens the ability of apurinic lesions to act as topoisomerase II poisons.

On the basis of these results, the tetrahydrofuran apurinic analogue was chosen as the model for structural studies. It provides a high degree of DNA cleavage stimulation, and unlike a natural apurinic site, it is subject to neither ring opening nor degradation by β-elimination.

Structure of a Topoisomerase II DNA Cleavage Site Containing an Apurinic Lesion. To characterize DNA distortions that are induced by topoisomerase II poisons, the structure of an apurinic lesion located within the context of a topoisomerase II DNA cleavage site was determined by NMR spectroscopy and compared to that of the wild-type sequence. Although structural information has been reported for apurinic sites in DNA, previous studies examined lesions in a completely different sequence context and did not analyze them for features relevant to the actions of topoisomerase II (*46*−*49*). Consequently, these studies provide little information regarding the potential effects of topoisomerase II poisons on enzyme activity.

The oligonucleotides used for the present study (represented by the sequence shown below) were duplex 12-mers that contained either a tetrahydrofuran apurinic analogue or a deoxyguanosine at residue 18. This residue (denoted by *X*) is located at the +2 position relative to the scissile phosphodiester bond (*arrow*) on the bottom strand of the topoisomerase II DNA cleavage site utilized for enzymology studies (see Figure 1).

```
     1  2  3  4 ↓5  6  7  8  9 10 11 12
5′- G  C  A  G  T  C  C  A  G  C  C  T -3′
3′- C  G  T  C  A  G  X  T  C  G  G  A -5′
    24 23 22 21 20 19 18 17↑16 15 14 13
```

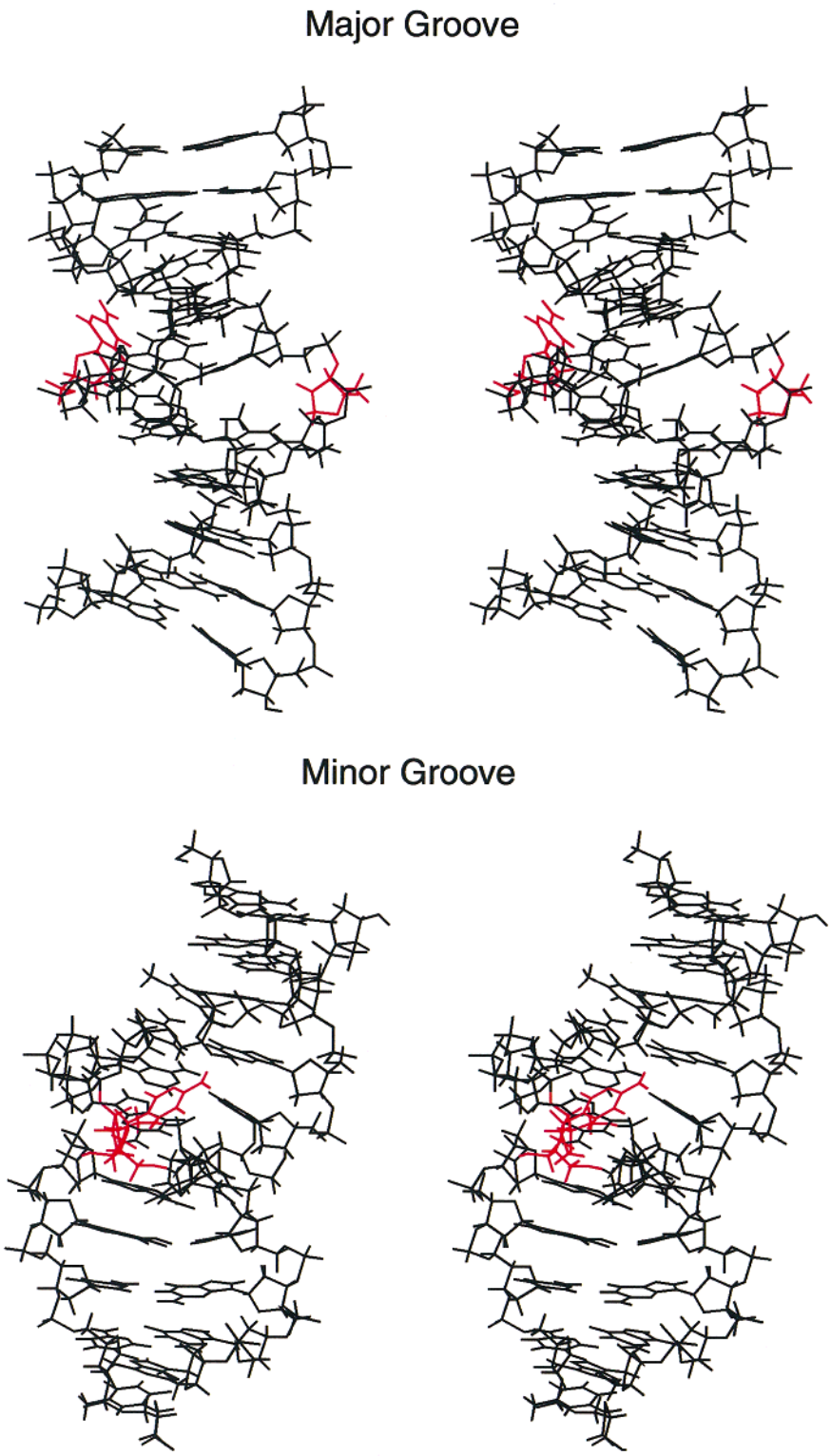

FIGURE 5: Stereoviews of the abasic dodecamer structure are shown with the major groove (*top*) or minor groove (*bottom*) prominent. The tetrahydrofuran apurinic analogue (X18) and the opposing deoxycytidine (C7) are depicted in *red*.

All NMR data were collected at 20 °C. Thermal stability of the abasic and wild-type dodecamers at this temperature was confirmed by 1D ^{1}H NMR, which revealed the expected number of sharp proton resonance peaks in the 7.0−8.2 ppm region of the spectrum (not shown). The proton chemical shift assignments for the wild-type and apurinic dodecamers, based on NOESY walks (Figures 3 and 4), are included in the Supporting Information.

Stereoviews looking into the major or minor groove of the apurinic dodecamer are shown in Figure 5. Spacefilling representations of both the apurinic and wild-type oligonucleotides are shown in Figure 6. The residue at position 18, as well as the complementary deoxycytidine (C7), are shown in *red*. A total of 12 convergent structures emerging from molecular dynamics calculations (6 each starting from A- and B-form models) were averaged to yield the refined

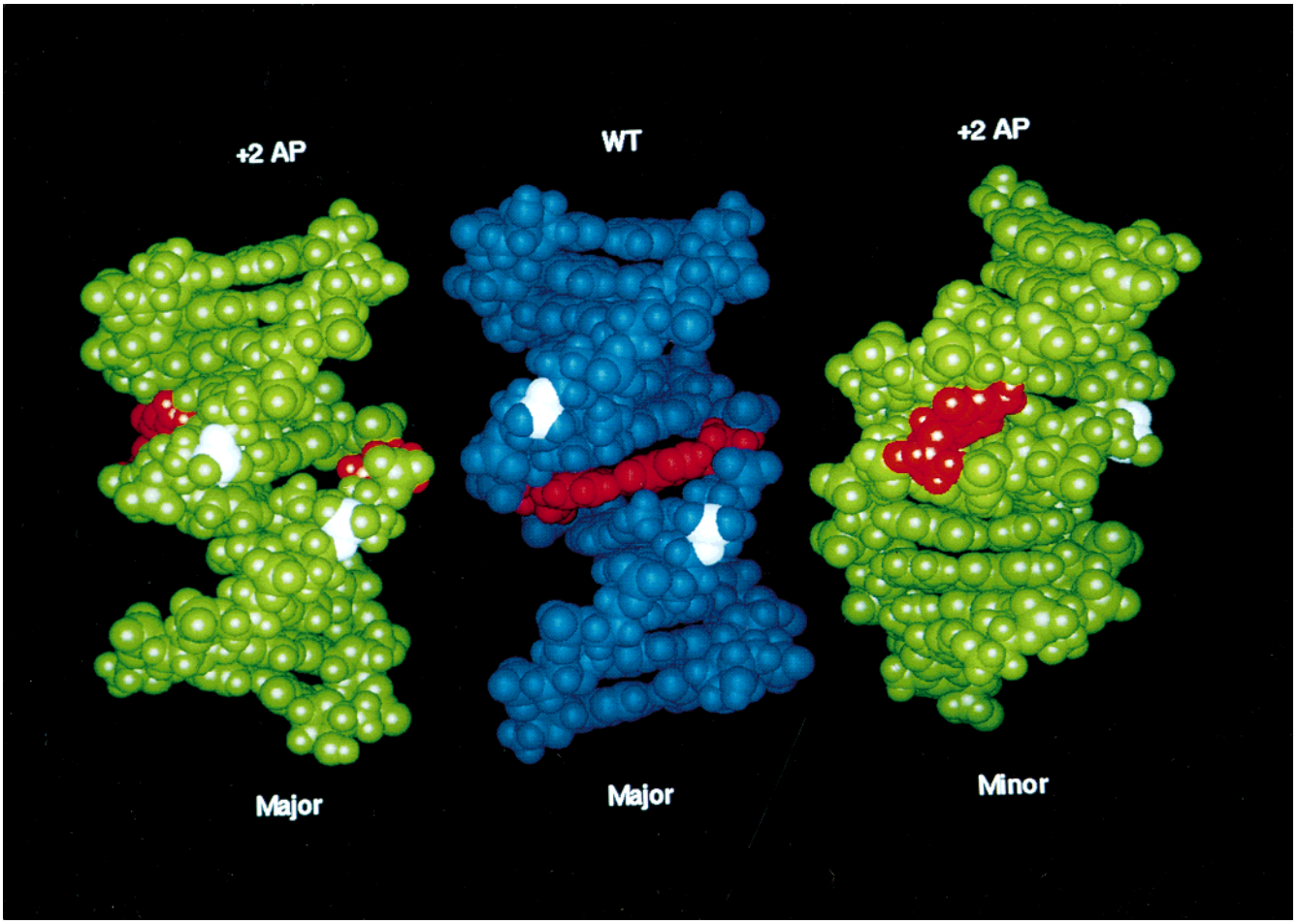

FIGURE 6: Spacefilling views looking at the major and minor grooves of the apurinic dodecamer (*+2 AP*, *left* and *right*, respectively, in *green*) and the major groove of the wild-type oligonucleotide (*WT*, center, in *blue*). The abasic tetrahydrofuran ring (X18) and the opposing deoxycytidine (C7) are shown in *red*, and the scissile phosphodiester bonds are in *white*.

structures of the apurinic and wild-type oligonucleotides (R_1^x = 0.095 and R_1^x = 0.077, respectively). An average pairwise rmsd of 1.65 and 1.31 Å were determined for the refined apurinic and wild-type structures, respectively.

The loss of the guanine at the +2 position on the bottom strand (X18) was confirmed by the loss of sequential NOE connectivity between anomeric and aromatic protons along this strand (compare the NOESY walks in Figures 3 and 4). The break in the NOESY walk between the +1 thymine (T17) and the +3 guanine (G19) reflects the absence of base stacking on the bottom strand. The elimination of base interactions at the apurinic site resulted in the expected upfield shift of the tetrahydrofuran ring protons relative to the deoxyribose protons of base-paired residues (see Supporting Information). The abasic site analogue has a pseudorotation angle near 350 degrees, indicating that the furanose ring adopts a C2′-exo conformation as compared to the C2′-endo conformation of deoxyribose rings in canonical B-form DNA.

Base stacking across from the apurinic site is disrupted, as the cytosine at the +3 position of the top strand (C7) is displaced into the minor groove (see Figures 5 and 6). The position of this cytosine was confirmed by NOE cross-peaks that indicated interactions of the cytosine H5 with both the H2 of the +4 adenine (A20) and the H1′ of the +5 deoxycytidine (C21) of the bottom strand (see Supporting Information). Furthermore, the cross-peak observed between the H1′ of the +3 deoxycytidine (C7) and the aromatic H8 proton of the adjacent adenine (A8) on the top strand was weak and disappeared at lower mixing times (see Figure 4).

Three major features distinguish the structure of the apurinic dodecamer from that of the wild-type oligonucleotide. All of these have the potential to alter interactions between topoisomerase II and its DNA substrate.

First, the loss of base stacking of the +3 cytosine (C7) across from the apurinic site collapsed the major groove in the central region of the topoisomerase II DNA cleavage site. This collapse had a profound effect on the spacial relationship between of the two scissile phosphodiester bonds that are attacked by the enzyme during its DNA cleavage reaction. These bonds (depicted in *white* in Figure 6) are located on opposite strands of the double helix and are ~15 Å across the major groove from one another in the wild-type structure. In the presence of the +2 apurinic lesion, the distance between the scissile bonds was reduced to ~11 Å. It has been suggested that during the catalytic cycle of topoisomerase II, the two active site tyrosyl residues must move a considerable distance (35−40 Å), and actually pass by each other, to achieve appropriate alignment with the points of cleavage on the DNA backbone (*50*). Consequently, it is possible that reducing the distance between the two scissile bonds could lower the activation energy for this process, and hence, accelerate the rate of scission.

Second, the presence of the apurinic lesion induced a bend in the docedamer that was centered about the topoisomerase II cleavage site. The bend angle was ~10 degrees relative to the axis of the wild-type duplex and was confirmed by electrophoretic mobility shift assays (not shown). Topoisomerase II displays an increased affinity for unusual DNA structures, such as crossovers, hairpins, tetraplexes, and bends (*51*−*54*). Moreover, the affinity of the enzyme for an oligonucleotide that contained a +2 apurinic site was ~3 times higher than it was for the corresponding unmodified DNA substrate (*29*). Since increases in topoisomerase II−DNA binding can lead to corresponding increases in DNA cleavage (*51*), bends induced by apurinic sites are likely to contribute to the enhanced DNA scission of substrates containing these lesions.

Third, the cytosine residue immediately opposite from the apurinic site was extrahelical and positioned in the minor groove of the dodecamer. Although it is not clear how distortions in the topography of the minor groove affect protein−DNA interactions, it is notable that many drugs that stimulate topoisomerase II-mediated DNA cleavage bind to nucleic acids through interactions with the minor groove (*55*−*58*).

In summary, when located at the +2 position of a topoisomerase II DNA cleavage site, an apurinic lesion that enhanced DNA scission ~20-fold reduced the distance between the scissile bonds, created a bend in the DNA backbone, and altered the topography of the minor groove. All of these features have the potential to influence topoisomerase II−DNA interactions. Although the present work cannot unambigiously assign the extent to which each individual alteration contributes to the poisoning of topoisomerase II, it provides novel insights into the structural distortions in DNA that are induced by topoisomerase II poisons. Furthermore, this study establishes a framework for the future analysis of nucleotide adducts and anticancer drugs that stimulate the DNA cleavage activity of topoisomerase II, and ultimately convert this essential enzyme to a lethal nuclease.

ACKNOWLEDGMENT

The authors are grateful to J. P. Weisenseel, M. Voehler, and Dr. S. L. Painter for their invaluable assistance with NMR spectroscopy and to J. M. Fortune and Dr. D. A. Burden for their critical reading of the manuscript.

SUPPORTING INFORMATION AVAILABLE

Proton chemical shift assignments for both structures, stereoviews of the wild-type dodecamer, and the region of the 2D NOESY spectrum containing NOE cross-peaks used in determining the minor groove position of C7 in the structure of the abasic dodecamer are available free of charge via the Internet at http://pubs.acs.org.

REFERENCES

1. Watt, P. M., and Hickson, I. D. (1994) *Biochem. J. 303*, 681−695.
2. Wang, J. C. (1996) *Annu. Rev. Biochem. 65*, 635−692.
3. Nitiss, J. L. (1998) *Biochim. Biophys. Acta 1400*, 63−81.
4. Burden, D. A., and Osheroff, N. (1998) *Biochim. Biophys. Acta 1400*, 139−154.
5. Wang, J. C. (1998) *Q. Rev. Biophys. 31*, 107−144.
6. Liu, L. F., Rowe, T. C., Yang, L., Tewey, K. M., and Chen, G. L. (1983) *J. Biol. Chem. 258*, 15365−15370.
7. Sander, M., and Hsieh, T. (1983) *J. Biol. Chem. 258*, 8421−8428.
8. Rowe, T. C., Chen, G. L., Hsiang, Y. H., and Liu, L. F. (1986) *Cancer Res. 46*, 2021−2026.
9. Zechiedrich, E. L., Christiansen, K., Andersen, A. H., Westergaard, O., and Osheroff, N. (1989) *Biochemistry 28*, 6229−6236.
10. Corbett, A. H., and Osheroff, N. (1993) *Chem. Res. Toxicol. 6*, 585−597.
11. Hickman, J. A. (1992) *Cancer Metastasis Rev. 11*, 121−139.
12. Nitiss, J. L., and Beck, W. T. (1996) *Eur. J. Cancer 32a*, 958−966.
13. Pommier, Y. (1997) in *Cancer Therapeutics: Experimental and Clinical Agents* (Teicher, B. A., Ed.) pp 153−174, Humana Press, Totowa, New Jersey.
14. Baguley, B. C., and Ferguson, L. R. (1998) *Biochim. Biophys. Acta 1400*, 213−222.
15. Kaufmann, S. H. (1998) *Biochim. Biophys. Acta 1400*, 195−211.
16. Kreuzer, K. N., and Cozzarelli, N. R. (1979) *J. Bacteriol. 140*, 424−435.
17. Chen, A. Y., and Liu, L. F. (1994) *Annu. Rev. Pharmacol. Toxicol. 34*, 191−218.
18. Liu, L. (1994) *Adv. Pharmacol. 29*.
19. Froelich-Ammon, S. J., and Osheroff, N. (1995) *J. Biol. Chem. 270*, 21429−21432.
20. Sinha, B. K. (1995) *Drugs 49*, 11−19.
21. Hande, K. R. (1998) *Biochim. Biophys. Acta 1400*, 173−184.
22. Gootz, T. D., and Brighty, K. E. (1996) *Med. Res. Rev. 16*, 433−486.
23. Drlica, K., and Zhao, X. (1997) *Microbiol. Mol. Biol. Rev. 61*, 377−392.
24. Hooper, D. C. (1998) *Biochim. Biophys. Acta 1400*, 45−61.
25. Freudenreich, C. H., and Kreuzer, K. N. (1994) *Proc. Natl. Acad. Sci. U.S.A. 91*, 11007−11011.
26. Marians, K. J., and Hiasa, H. (1997) *J. Biol. Chem. 272*, 9401−9409.
27. Capranico, G., and Binaschi, M. (1998) *Biochim. Biophys. Acta 1400*, 185−194.
28. Kingma, P. S., and Osheroff, N. (1998) *Biochim. Biophys. Acta 1400*, 223−232.
29. Kingma, P. S., and Osheroff, N. (1997) *J. Biol. Chem. 272*, 1148−1155.
30. Kingma, P. S., and Osheroff, N. (1997) *J. Biol. Chem. 272*, 7488−7493.
31. Kwok, Y. and Hurley, L. H. (1998) *J. Biol. Chem. 273*, 33020−33026.
32. Kwok, Y. and Hurley, L. H. (1998) *Proc. Natl. Acad. Sci. U.S.A. 95*, 13531−13536.
33. Kingma, P. S., Corbett, A. H., Burcham, P. C., Marnett, L. J., and Osheroff, N. (1995) *J. Biol. Chem. 270*, 21441−21444.
34. Felix, C. A., Lange, B. J., Hosler, M. R., Fertala, J., and Bjornsti, M. (1995) *Cancer Res. 55*, 4287−4292.
35. Kingma, P. S., Greider, C. A., and Osheroff, N. (1997) *Biochemistry 36*, 5934−5939.
36. Moe, J. G., Reddy, G. R., Marnett, L. J., and Stone, M. P. (1994) *Chem. Res. Toxicol. 7*, 319−328.
37. Jones, W. J., Johnston, D. S., and Stone, M. P. (1998) *Chem. Res. Toxicol. 11*, 873−881.
38. Arnott, S., and Hukins, D. W. L. (1972) *Biochem. Biophys. Res. Commun. 47*, 1504−1509.
39. Arnott, S., and Hukins, D. W. L. (1973) *J. Mol. Biol. 81*, 93−105.
40. Borgias, B. A., and James, T. L. (1990) *J. Magn. Reson. 87*, 475−487.
41. Keepers, J. W., and James, T. L. (1984) *J. Magn. Reson. 57*, 404−426.
42. Brunger, A. T. (1992), Yale University Press, New Haven, CT.

43. Weisenseel, J. P., Moe, J. G., Reddy, G. R., Marnett, L. J., and Stone, M. P. (1995) *Biochemistry 34*, 50−64.
44. Ravishankar, G., Swaminathan, S., Beveridge, D. L., Lavery, R., and Sklenar, H. (1989) *J. Biomol. Struct. Dyn. 6*, 669−699.
45. Friedberg, E. C., Walker, G. C., and Siede, W. (1995) *DNA Repair and Mutagenesis*, 2nd ed., American Society for Microbiology Press, Washington D. C.
46. Raap, J., Dreef, C. E., van der Marel, G. A., van Boom, J. H., and Hilbers, C. W. (1987) *J. Biomol. Struct. Dyn. 5*, 219−247.
47. Cuniasse, P., Fazakerley, G. V., and Guschlbauer, W. (1990) *J. Mol. Biol. 213*, 303−314.
48. Coppel, Y., Berthet, N., Coulombeau, C., Coulombeau, C., Garcia, J., and Lhomme, J. (1997) *Biochemistry 36*, 4817−4830.
49. Berger, R. D., and Bolton, P. H. (1998) *J. Biol. Chem. 273*, 15565−15573.
50. Berger, J. M., Gamblin, S. J., Harrison, S. C., and Wang, J. C. (1996) *Nature 379*, 225−232.
51. Zechiedrich, E. L., and Osheroff, N. (1990) *EMBO J. 9*, 4555−4562.
52. Howard, M. T., Lee, M. P., Hsieh, T. S., and Griffith, J. D. (1991) *J. Mol. Biol. 217*, 53−62.
53. Chung, I. K., Mehta, V. B., Spitzner, J. R., and Muller, M. T. (1992) *Nucleic Acids Res. 20*, 1973−1977.
54. Froelich-Ammon, S. J., Gale, K. C., and Osheroff, N. (1994) *J. Biol. Chem. 269*, 7719−7725.
55. Nelson, E. M., Tewey, K. M., and Liu, L. F. (1984) *Proc. Natl. Acad. Sci. U.S.A. 81*, 1361−1365.
56. Frederick, C. A., Williams, L. D., Ughetto, G., van der Marel, G. A., van Boom, J. H., Rich, A., and Wang, A. H.-J. (1990) *Biochemistry 29*, 2538−2549.
57. Singh, M. P., Hill, G. C., Peoc′h, D., Rayner, B., Imbach, J. L., and Lown, J. W. (1994) *Biochemistry 33*, 10271−10285.
58. Ismail, M. A., Sanders, K. J., Fennell, G. C., Latham, H. C., Wormell, P., and Rodger, A. (1998) *Biopolymers 46*, 127−143.

BI991750S